Cellular Uptake of the ATSM–Cu(II) Complex under Hypoxic Conditions

Gulshan R. Walke, Shelly Meron, Yulia Shenberger, Lada Gevorkyan-Airapetov, and Sharon Ruthstein*[a]

The Cu(II)-diacetyl-bis (N4-methylthiosemicarbazone) complex (ATSM–Cu(II)) has been suggested as a promising positron emission tomography (PET) agent for hypoxia imaging. Several in-vivo studies have shown its potential to detect hypoxic tumors. However, its uptake mechanism and its specificity to various cancer cell lines have been less studied. Herein, we tested ATSM–Cu(II) toxicity, uptake, and reduction, using four different cell types: (1) mouse breast cancer cells (DA-3), (2) human embryonic kidney cells (HEK-293), (3) breast cancer cells (MCF-7), and (4) cervical cancer cells (Hela) under normoxic and hypoxic conditions. We showed that ATSM–Cu(II) is toxic to breast cancer cells under normoxic and hypoxic conditions; however, it is not toxic to normal HEK-293 non-cancer cells. We showed that the Cu(I) content in breast cancer cell after treatment with ATSM–Cu(II) under hypoxic conditions is higher than in normal cells, despite that the uptake of ATSM–Cu(II) is a bit higher in normal cells than in breast cancer cells. This study suggests that the redox potential of ATSM–Cu(II) is higher in breast cancer cells than in normal cells; thus, its toxicity to cancer cells is increased.

1. Introduction

Cancer cells are metabolically more active and hence, more proliferative than normal cells.[1] The increase in the blood supply to the malignant tumors was found to fulfill the cells' increased oxygen demand.[2] Therefore, based on the intracellular oxygen levels, malignant cells can easily be differentiated from normal cells. The onset of hypoxia in cells is one of the essential biomarkers in cancer.[3] Moreover, cardiological and neurological disease conditions have also been reported to influence the cellular oxygen levels.[4] Hypoxia is a condition that affects cells with lower oxygen levels (median $pO_2 < 5$ mm Hg).[5] In comparison, normal tissues have oxygen levels with a median pO_2 value of 40–60 mm Hg.[6] Therefore, hypoxic tissues exhibit a highly reducing intracellular milieu.[6] Hypoxic cells are resistant to chemotherapy and are detrimental to cell recovery because oxygen is required for the recovery of the radio-damaged DNA.[7]

The development of hypoxia-selective radiotracers that can be easily monitored using positron emission tomography (PET) has emerged as a demanding task in nuclear medicine. One of the most common hypoxic biomarkers is ^{18}F-Fluoromisonidazole (^{18}FMISO), a nitroimidazole derivative.[8] Under low oxygen conditions, the nitrogen dioxide group in ^{18}FMISO is reduced to the amine group and then is easily trapped by cellular proteins; the retention time of ^{18}FMISO increases in hypoxic tissues.[8b,9] The main disadvantage of using the ^{18}F radioactive isotope lies in its short half-life: 109.7 min; after its injection to obtain a sufficient signal, the waiting period is about 1.5 h. The development of novel biomarkers to diagnose hypoxic conditions opens up new avenues for researchers studying cancer and neurodegenerative diseases.

Recently, metal-based complexes have been studied for their high selectivity towards hypoxic tissues, based on their redox ability. Copper-based (^{60}Cu, ^{61}Cu, ^{62}Cu, ^{64}Cu, or ^{67}Cu) radiotracers were examined to diagnose hypoxic cells.[10] Among the Cu(II) complexes, the Cu(II)-diacetyl-bis(N4-methylthiosemicarbazone) complex (ATSM–Cu(II), Scheme 1), has been proposed as a promising PET agent for hypoxia imaging.[10b,d] The advantage of using the radioactive isotope of copper, ^{64}Cu(II) lies in its half-life of 12.8 h, which provides enough time for cellular uptake and post-injection analysis. ATSM–Cu(II) is a low molecular weight, membrane-permeable copper complex. Several *in-vivo* studies have reported the greater uptake and retention of ATSM–Cu(II) occurring in hypoxic tumor tissues.[11]

The cellular uptake mechanism underlying ATSM–Cu(II) may not involve copper transport proteins.[12] Once ATSM–Cu(II)

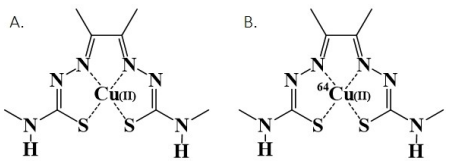

Scheme 1. Structure of the ATSM–Cu(II) complex (A) and the ATSM–Cu(II) complex with radio-isotope ^{64}Cu(II) (B).

[a] *Dr. G. R. Walke, S. Meron, Dr. Y. Shenberger, Dr. L. Gevorkyan-Airapetov, Prof. S. Ruthstein*
Department of Chemistry, Faculty of Exact Sciences, and the Institute for Nanotechnology and advanced materials (BINA)
Bar-Ilan University
5290002 Ramat-Gan (Israel)
E-mail: Sharon.ruthstein@biu.ac.il

Supporting information for this article is available on the WWW under https://doi.org/10.1002/open.202100044

enters the cell, the dissociation rate of copper from ATSM ligands largely depends upon the cellular oxygen levels. In normoxic cells, ATSM–Cu(II), having a low redox potential, is not reduced to the Cu(I) or ATSM–Cu(I) intermediate; hence, it is not retained intracellularly (by proteins/peptides) and it is readily washed out of the cells. On the other hand, due to the aggressive reducing conditions, hypoxic cells facilitate the reduction of ATSM–Cu(II). The redox cycling of ATSM–Cu(II) takes place through the intermediate ATSM–Cu(I); loosely held Cu(I) dissociates from the ATSM coordination sphere via cellular proteins (precipitated as copper sulfides); thus, it is retained by the cells.[13] Therefore, the reduction, dissociation, and re-oxidation of ATSM–Cu(II) play a critical role in diagnosing the hypoxic cells. However, the continuous shuttling of redox-active copper in (I) to (II) or vice versa catalyzes Fenton-like reactions that produce different reactive oxygen species (ROS), which can damage biomolecules such as DNA, RNA, proteins, and more.[14] Therefore, it was suggested that copper complexes also have therapeutic potential in various cancer models.[15] Indeed, several thiosemicarbazone-based Cu(II) complexes were tested, and showed promising activity as cancer drugs.[16]

ATSM–Cu(II) complex's cellular uptake may depend upon the cell type and the intracellular oxygen levels. The ATSM–Cu-(II) complex is clinically relevant because it can detect hypoxic tumors; however, the human prostate cancer cells' imaging might be limited by the over-expression of fatty acid synthase in prostate cancer malignancies.[17]

Despite tremendous efforts, the cellular uptake of ATSM–Cu(II) remains unclear. An intriguing question is whether the uptake of ATSM–Cu(II) depends upon the cell types or the cellular oxygen levels when modulating the cellular uptake of the ATSM–Cu(II) complex.

The present study demonstrates the cytotoxicity effect of ATSM–Cu(II) in four different mammalian cell lines under both normoxic and hypoxic conditions. The intracellular copper content was measured using a well-known Cu(I) chelator, bicinchoninic acid (BCA), under normoxic and hypoxic conditions. In addition, *in-vitro* experiments using the radio-labeled ATSM–^{64}Cu(II) were carried out to obtain more insight into intracellular copper transport. Finally, we performed western blots to detect the expression level of CTR1 copper transporter at various cell lines, and determine whether a correlation exists between the ATSM–Cu(II) uptake and the cellular copper metabolism.

2. Results and Discussion

Initially, we tested ATSM–Cu(II) and Cu(II) cytotoxicity against four different cell lines: (1) mouse breast cancer cells-DA-3, (2) human embryonic kidney cells-HEK-293, (3) breast cancer cells-MCF-7, and (4) cervical cancer cells-Hela under normoxic and hypoxic conditions for 24 h using the MTT assay (Figure 1). To achieve hypoxic conditions, the cells were kept in an air-tight box containing hypoxic bags, this creates conditions whereby $O_2 < 0.1\,\%$ within 2.5 h. In all the cell experiments, $CuCl_2$ salt was used and is referred to as a Cu(II). The toxicity of Cu(II) alone against ATSM–Cu(II) was comparable under both normoxic and hypoxic conditions. In all cell experiments with ATSM–Cu(II), the DMSO percentage was less than 1% (except 1% for the 1 mM concentration). With this concentration of DMSO, there was no significant effect on cell viability. Table 1 presents the IC50 values for Cu(II) and ATSM–Cu(II) for different cell lines. The IC50 values were calculated using the Ed50v10 Excel sheet function.

In the DA-3 cell lines, the ATSM–Cu(II) complex shows an IC50 value of about 298.0 ± 18.7 μM under normoxic conditions, which is less than that of free Cu(II). On the other hand, under hypoxic conditions, ATSM–Cu(II) was found to be highly toxic against DA-3 cells (< 50 μM). For HEK-293 cells, Cu(II) alone shows more toxicity than the ATSM–Cu(II) complex under normoxic and hypoxic conditions. The treatment of ATSM–Cu(II) to HEK-293 cells did not significantly kill the cells up to a concentration of 0.5 mM (about 90% cell viability) under hypoxic conditions. In addition, the complex does not significantly affect the cell viability of HEK-293 under normoxic conditions. The complexation of Cu(II) by the ATSM ligand alters the toxicity of copper towards the HEK-293 cells. In the case of MCF-7 cells, ATSM–Cu(II) was found to be toxic at all concentrations (at least above 50 μM) irrespective of the experimental conditions. Copper alone (Cu(II)) was found to be non-toxic at higher concentrations (until 1 mM) to MCF-7 cells under normal conditions, whereas a significant decrease in cell viability (nearly 50%) was observed above a concentration of 0.5 mM under hypoxic conditions. For Hela cells, Cu(II) shows IC50 values above 500 μM under normoxic and hypoxic conditions. In comparison, complexed Cu(II) exhibits slightly more toxicity than Cu(II) towards Hela cells under normoxic conditions. Interestingly, ATSM–Cu(II) exhibits more cell viability under hypoxic than under normoxic conditions. Overall, the data indicate that the ATSM–Cu(II) complex shows more toxicity towards cancerous cell lines DA-3 and MCF-7, except for Hela, than do normal cells HEK-293. In addition, the ATSM–Cu(II) complex can be slightly non-toxic to cancerous cells (DA-3 cells)

Table 1. IC50 values of the Cu(II) and ATSM–Cu(II) complex in different cells under normoxic and hypoxic conditions. All data are representative of three similar experiments and the IC50 value represents the mean ± SEM.

Type of Cells		DA-3	HEK-293	MCF-7	Hela
Normoxic	IC50 for Cu(II) [μM]	440.0 ± 6.8	158.0 ± 10.2	> 1000	628.5 ± 12.2
	IC50 for ATSM–Cu(II) [μM]	298.0 ± 18.7	> 1000	< 50	341.4 ± 4.9
Hypoxic	IC50 for Cu(II) [μM]	395.4 ± 1.7	385.0 ± 8.2	607.8 ± 17.1	554.6 ± 17.7
	IC50 for ATSM–Cu(II) [μM]	< 50	> 1000	< 50	745.1 ± 15.9

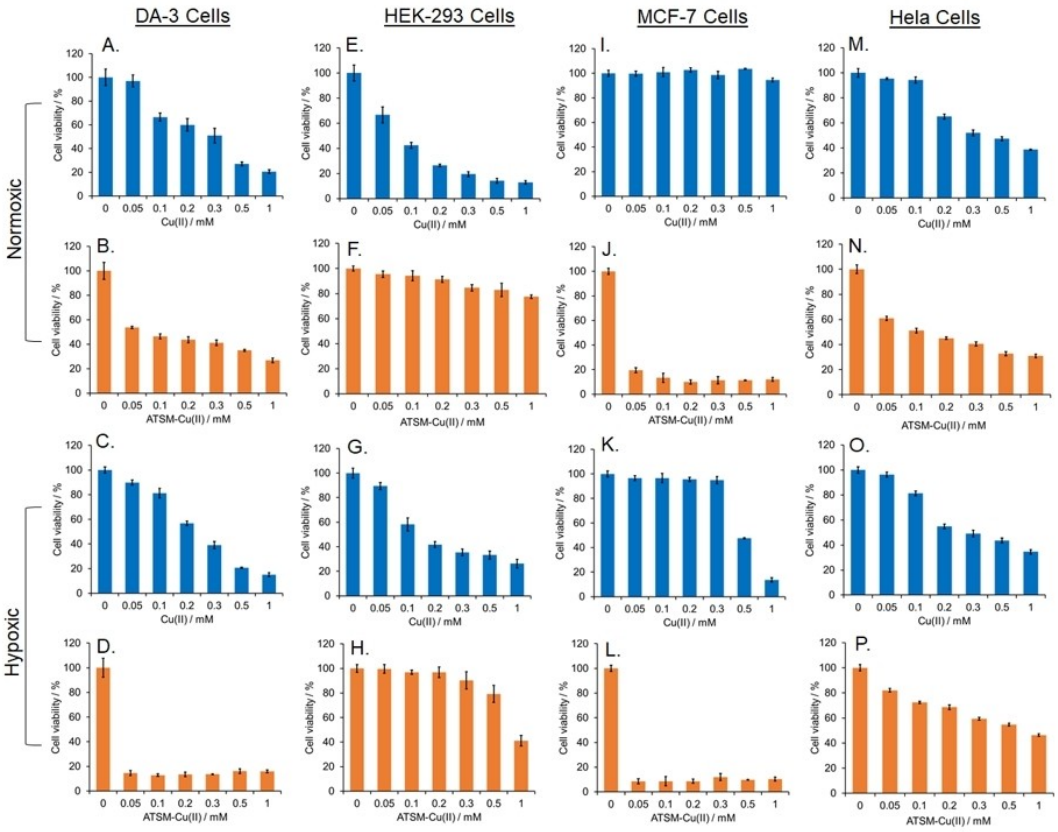

Figure 1. Cell viability measurement using the MTT assay under normoxic conditions (above) and the hypoxic conditions (below) for DA-3 cells (A, B, C, and D), HEK-293 (E, F, G, and H), MCF-7 cells (I, J, K, and L), and Hela cells (M, N, O, and P).

under normal conditions. However, under both normoxic and hypoxic conditions, the complex is highly toxic (IC50 value <50 μM) to breast cancer cells, MCF-7.

To compare the rate of copper uptake by normal cells and cancerous cells, we analyzed the copper uptake and reduction in HEK-293 and MCF-7 cells using a bicinchoninic acid (BCA) ligand - a Cu(I) selective chromophore. BCA binds Cu(I) with high affinity in a 2:1 stoichiometry, forming the $(BCA)_2$–Cu(I) complex.[18] The formation of the $(BCA)_2$–Cu(I) complex can be evaluated by following an intense absorption peak at 562 nm, with an extinction coefficient of 7700 M^{-1}.[18a] We treated cells with Cu(II) and the ATSM–Cu(II) complex and also subjected them to normoxic and hypoxic conditions. The absorbance at 562 nm, obtained for the control cells, was subtracted from the absorbance obtained after treatment of Cu(II) or ATSM–Cu(II) for a specific time. Thus, the innate intracellular Cu(I) and Cu(I) acquired from the medium can be excluded. The concentration of the $(BCA)_2$–Cu(I) complex can be calculated using Beer-Lamberts law. The concentration of $(BCA)_2$–Cu(I) represents the concentration of the intracellular Cu(I) content. Since, ATSM–Cu(II) is highly toxic to MCF-7 cells (IC50 <50 μM) we used the optimal concentration of 10 μM for both Cu(II) and ATSM–Cu(II) treatment to achieve reproducible results. Upon treatment with 10 μM of the ATSM–Cu(II) complex, significant cell death was observed after 6 h. Therefore, we monitored the intracellular Cu(I) levels up to 3 h. Figure 2 presents the intracellular Cu(I) content at times of 0.5 h, 1 h, and 3 h.

An elevation in the Cu(I) levels with respect to time was observed in controls (cells without treatment), Cu(II), and in ATSM–Cu(II) complex-treated cells (see SI, Figure S1). The cell medium (the complete DMEM) contains copper (Cu(II)/Cu(I)) in trace amounts. The small elevation in Cu(I) levels in controls is probably due to the copper uptake from the cell medium, along with the intracellular Cu(I) content. However, the increased copper is statistically insignificant.

In HEK-293 cells, a gradual increase in the cellular Cu(I) content was observed until 24 h under normoxic and hypoxic conditions (Figure 2A; see SI, Figure S2). At 3 h and 24 h, after Cu(II) treatment under normoxic conditions, the cellular Cu(I) concentration was found to be 0.77 μM and 3.11 μM, respectively. Under hypoxic conditions, an increase in Cu(I) content was found with 1.49 μM after 3 h and 4.02 μM after 24 h. The hypoxic conditions may accelerate the reduction of the Cu(II), which results in increased intracellular Cu(I) content.

Similarly, in the case of ATSM–Cu(II) in HEK-293 cells, a gradual elevation in the intracellular Cu(I) levels was observed at the early time intervals. The maximum Cu(I) content was found at 3 h (see SI, Figure S2). In addition, the Cu(I) concentration was much higher for ATSM–Cu(II) than for free Cu(II), suggesting that the uptake of ATSM–Cu(II) by the cells is higher than that of the free Cu(II) ions. The maximum Cu(I) concen-

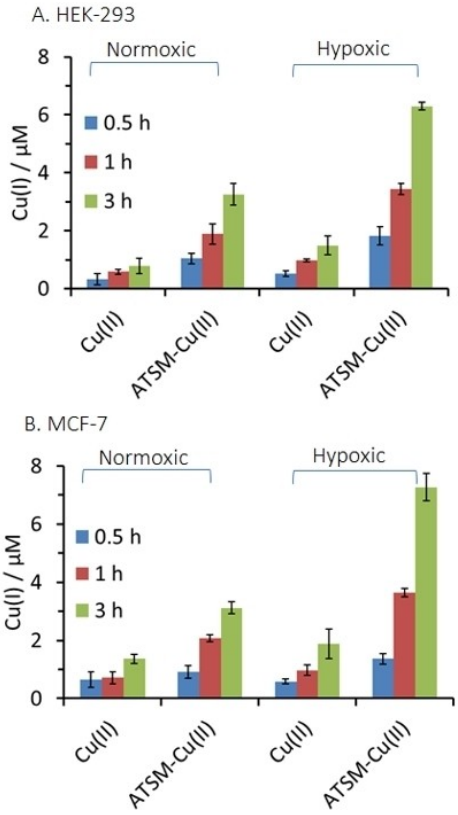

Figure 2. Intracellular Cu(I) content upon the time-dependent treatment of 10 μM Cu(II) or ATSM–Cu(II), measured using BCA ligand under normoxic and hypoxic conditions in A. HEK-293 cells, and B. MCF-7 cells. The values are expressed as the means ± SEM of at least three independent experiments.

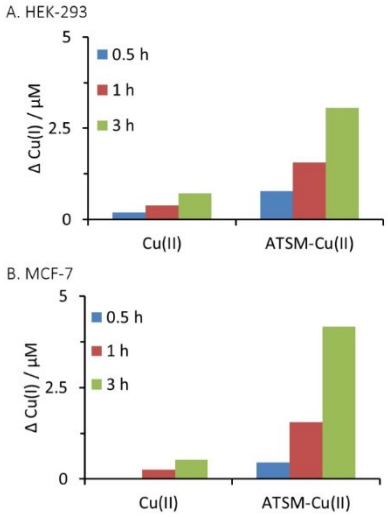

Figure 3. The difference in the intracellular Cu(I) content between hypoxic and normoxic conditions upon time-dependent treatment of 10 μM Cu(II) or ATSM–Cu(II), measured using BCA ligand in A. HEK-293 cells, and B. MCF-7 cells.

tration at 3 h was found to be 3.25 μM under normoxic conditions and 6.3 μM under hypoxic conditions. At later time intervals (6 h and 24 h), a slight reduction in the Cu(I) levels was detected, whereas at 24 h, under normoxic conditions, the Cu(I) content was found to be 3.3 μM; however, under hypoxic conditions it was 4.6 μM. This suggests a rapid depletion of ATSM–Cu(II) from HEK-293 cells.

A similar experiment was carried out on MCF-7 breast cancer cells (Figure 2B). After 3 h, under normoxic and hypoxic conditions, the Cu(I) concentration after treatment with Cu(II) was found to be 1.36 μM and 1.88 μM, respectively, which suggestsonly a minor increase in Cu(I) content between normoxic and hypoxic conditions. However, the Cu(I) content after treatment with ATSM–Cu(II) complex in MCF-7 cells was found to be much higher, whereas under normoxic conditions at 3 h, a concentration of 3.1 μM Cu(I) was found, and 7.2 μM was found under hypoxic conditions. Similar to the HEK-293 cells, in MCF-7 cells, an increased cellular Cu(I) content was observed more under hypoxic conditions than under normoxic conditions as expected, owing to the low oxygen level in the cells, which accelerates the reduction of Cu(II) to Cu(I). However the concentration of Cu(I) after ATSM–Cu(II) treatment in MCF-7 cells under hypoxic conditions was much higher than under normoxic conditions. Figure 3 shows the difference in Cu(I) concentration between hypoxic and normoxic conditions for both cell types after Cu(II) and ATSM–Cu(II) treatment. After 3 h of Cu(II) treatment using both cell types, there was only a slight change in the Cu(I) concentration, owing to the hypoxic conditions. However, after treatment with ATSM–Cu(II), the Cu(I) content increased by four times in the HEK-293 cells and about eight times in MCF-7 cells, compared with treatment with free Cu(II) ions. Moreover, there was 14% more Cu(I) concentration in MCF-7 cells than in the HEK-293 cells under hypoxic conditions. The large increase in Cu(I) content in MCF-7 cells under hypoxic conditions may affect the toxicity of this complex to the cells.

Overall, the results indicate that ATSM–Cu(II) integrates into both the HEK-293 and MCF-7 cells. The rate of the cellular uptake of ATSM–Cu(II) is higher than that of free Cu(II) in both cell types.

The intracellular oxygen levels influence the cellular copper transport and reduction (for both free Cu(II) and ATSM–Cu(II)), since more Cu(I) is integrated into the cells under hypoxic conditions than under normoxic conditions.

To compare the cellular copper uptake into the cells upon Cu(II) and ATSM–Cu(II) treatment, we performed ^{64}Cu(II) radioactive experiments in HEK-293 and MCF-7 cells using a radioactive isotope of copper, ^{64}Cu(II). These experiments evaluate the content of ^{64}Cu, which contains both ^{64}Cu(II) and the reduced form, ^{64}Cu(I). Previously, the copper uptake studies on the EMT6 cells over time under different oxygen concentrations (0%, 0.1%, 0.5%, 5%, and 20%) showed that the maximum uptake was at 1 h after injection of ATSM–^{64}Cu(II) (about 70–90% for 0.1 to 0% oxygen).[19] However, regarding ATSM–Cu(II), the maximum Cu(I) concentration measured using BCA, was observed at 3 h post-treatment. Therefore, the cellular uptake in the HEK-293 and MCF-7 cells was tested using the radiolabeled complex at 1 h and 3 h post-injection (Figure 4). At the time

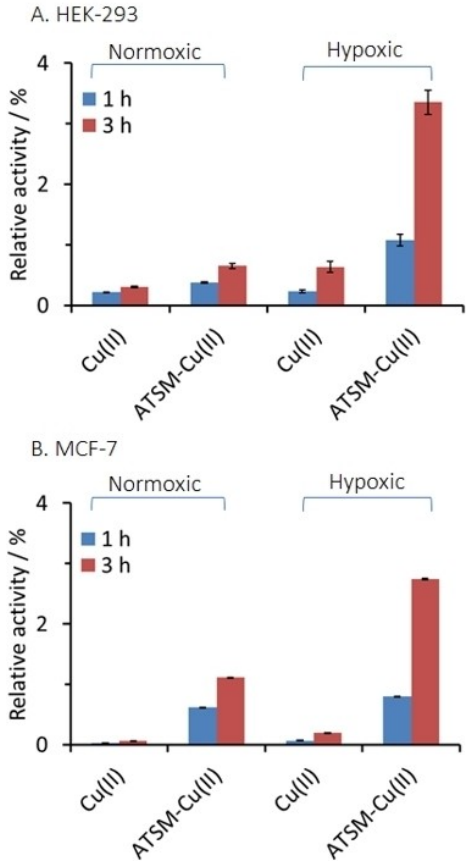

Figure 4. Intracellular ^{64}Cu content in HEK-293 cells A. and MCF-7 cells B. measured using a radioactive isotope of copper, ^{64}Cu(II), and ATSM–^{64}Cu(II) under normoxic and hypoxic conditions.

that ^{64}Cu(II) and ATSM–^{64}Cu(II) were injected, the activities were 4.67 μCi and 5.29 μCi, respectively. The activity of the radioisotope integrated into the cells was plotted as the percentage of the relative activity using the activity at the time of the injection. The results obtained are in agreement with those in the non-radiolabeled cell experiments. In both cell types, the uptake of ATSM–^{64}Cu(II) is significantly higher than that of ^{64}Cu(II) under both normoxic and hypoxic conditions for times of 1 h and 3 h (Figure 4), and it is much higher at 3 h than at 1 h after injection. Under hypoxic conditions, ^{64}Cu(II) or ATSM–^{64}Cu(II) integrated more easily in HEK-293 and MCF-7 cells than under normoxic conditions. In HEK-293 cells, ATSM–^{64}Cu(II) shows the highest percentage activity, 3.35% at 3 h, which is about 3.5 times higher than the percentage activity (1.07%) observed at 1 h under hypoxic conditions. When we compare the percentage of the relative activity of ATSM–^{64}Cu(II) at 3 h under normoxic and hypoxic conditions, the uptake of the complex under hypoxic conditions was found to be ~5.1 times higher than the uptake under normoxic conditions.

Similarly, in MCF-7 cells, higher activity was observed with ATSM–^{64}Cu(II)-treated cells than with ^{64}Cu(II)-treated cells under both normoxic and hypoxic conditions. Under hypoxic conditions, ATSM–^{64}Cu(II) shows the highest percentage activity, 2.75% at 3 h, which is 3.4 times higher than the percentage activity at 1 h (0.79%) under hypoxic conditions and also about 2.5 times higher than the percentage activity (1.1%) observed at 3 h under normoxic conditions. Surprisingly, the uptake of the complex in HEK-293 cells was found to be slightly higher than in MCF-7 cells under normoxic conditions.

The experiments performed so far suggest that the ATSM–Cu(II) complex is much more toxic to MCF-7 cells than to HEK-293 cells. We detected higher Cu(I) content after 3 h of treatment and under hypoxic conditions for MCF-7 cells than for HEK-293 cells. However, the uptake of ATSM–Cu(II) in HEK-293 cells is 20% higher than in MCF-7 cells (based on the radioactive experiments). In order to determine whether this difference between the cell types is related to a different copper metabolism in the various cell types, we performed western blots to evaluate the amount of the main copper transporter, CTR1, in the HEK-293, MCF-7, and Hela cells (Figure 5). The experiment indicated that the CTR1 expression level is the highest in HEK-293 cells, and that it is the lowest in Hela cells. The higher amount of CTR1 in HEK-293, compared with MCF-7 might explain why ATSM–Cu(II) uptake is higher in HEK-293 cells than in MCF-7 cells. In addition, this experiment also proposes that the ATSM–Cu(II) uptake in Hela cell is very low owing to the low amount of CTR1; therefore, probably ATSM–Cu(II) is less toxic to Hela than to MCF-7 cells.

3. Conclusions

Herein, we explored the cellular update and toxicity in various cell systems of the radiotracer ATSM–Cu(II). We showed that ATSM–Cu(II) is more toxic to breast cancer cell lines than to normal HEK-293 cells; however, its toxicity to Hela cancer cells is lower than in the breast cancer cell lines. This indicates that Cu(II) complexes do not have a similar effect in different cancer cells. Moreover, ATSM–Cu(II) toxicity increased under the hypoxic conditions of the cell. We also showed that the Cu(I) content after ATSM–Cu(II) treatment is higher in breast cancer cells than in normal cells, despite that the uptake of ATSM–Cu(II) is higher in normal cells (HEK-293) than in breast cancer MCF-7 cells. This suggests that the toxicity of ATSM–Cu(II) is associated with a reduction of Cu(II) to the toxic reduced form Cu(I). We also found that the amount of CTR1 copper transporter is higher in HEK-293 cells than in MCF-7 cells, and that it is the lowest in Hela cells. This suggests that the ATSM–Cu(II)

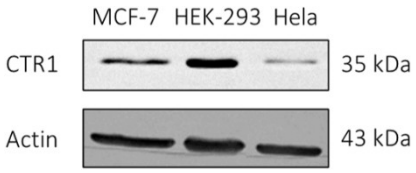

Figure 5. Expression of copper transporters, CTR1, in several cell lines by Western blot analysis. Actin was used as a loading control.

uptake and toxicity may be correlated with the cells' copper metabolism.

Experimental Section

Materials and Methods

All chemicals obtained were of high-quality grade and used without further purification. 4-Methyl-3-thiosemicarbazide, diacetyl (2,3-butanedione), $Cu(Cl)_2 \cdot 2H_2O$, bicinchoninic acid (BCA), and sterile-filtered cell culture grade dimethyl sulfoxide (DMSO) were purchased from Sigma-Aldrich.Dulbecco's Modified Eagle's Medium (DMEM). Fetal Bovine Serum (FBS), antibiotic (penicillin and streptomycin) solution, and MTT (3-(4, 5-Dimethylthiazol-2-yl)-2,5-diphenyltetrazolium bromide) were purchased from Himedia. Hypoxic bags were purchased from Sigma-Aldrich. $^{64}CuCl_2$ was obtained from Acom-srl, Italy.

Synthesis of the ATSM–Cu(II) Complex

We used a previously reported method for the synthesis of the ATSM–Cu(II) complex.[12b,20]

First, the ATSM ligand was synthesized by the condensation reaction of 4-methyl-3thiosemicarbazide (1.2 g, 11.4 mmol) and diacetyl (0.5 mL, 5.7 mmol) in ethanol (50 mL) with constant heating and stirring. A few drops of glacial acetic acid were added to the reaction mixture and then it was refluxed at 60 °C for 4 h. A white precipitate was formed. The flask was kept at 4 °C overnight for complete precipitation. Finally, a pale-yellow precipitate was obtained, then washed 3–4 times with ethanol and diethyl ether. ^{1}H-NMR (DMSO-d6): 10.22(s,2H) NH, 8.38 (m,2H) $NHCH_3$, 3.02 (d, 6H) $NHCH_3$, 2.20 (s, 6H) 2xCH_3 and ESI-MS (+): m/z 260.4.

ATSM–Cu(II) complex: ATSM ligand (0.1 g, 0.38 mmol) was dissolved in ethanol with constant heating and stirring. An ethanolic solution of copper acetate (0.0768 g, 0.38 mmol) was added dropwise to the ligand solution. A brown precipitate formed immediately. The reaction mixture was refluxed at 60 °C for 4 h and again was refluxed overnight at room temperature. The brown-red precipitate obtained was washed several times with ethanol and diethyl ether. UV-visible spectroscopy: λ_{max} (DMSO) at 311 nm and 355sh, 476 nm and 525sh. ESI-MS (+): m/z 322.

Stock Solution Preparation

A stock solution of ATSM–Cu(II) (100 mM) was prepared in DMSO. A stock solution of $CuCl_2$ (100 mM) was prepared in distilled water and the concentration was verified by UV-Vis spectroscopy from the d-d band of Cu(II) at 780 nm ($\varepsilon = 12\ M^{-1}\ cm^{-1}$). These stock solutions were further diluted and used for the experiments listed below.

Cell Viability Measurement Using MTT

Cells were grown in DMEM medium supplemented with 10% FBS, 1% L-glutamine, and 1% antibiotic solution (penicillin and streptomycin) at 37 °C in a humidified chamber at 5% CO_2. The samples (different concentrations of Cu(II) and the ATSM–Cu(II) complex) were passed through 0.22 K_d syringe filters for sterilization before treatment. Cell viability was measured in 96-well plates by a quantitative colorimetric assay using MTT in triplicate. Briefly, 10^5 cells per ml were seeded in 96-well plates for the assay. The cells were treated with samples in DMEM medium without FBS (treatment media). The treatment media were prepared using a 100 mM stock solution of Cu(II) and ATSM–Cu(II). For ATSM–Cu(II), the treatment medium contained less than 1% DMSO (except the 1 mM concentration containing 1% DMSO). At 24 h after the treatment, the media were removed, 20 μl 5 mg/ml MTT (the final concentration) was added to the wells, and the cells were incubated at 37 °C for another 4 h. The MTT solution was removed, and the colored formazan crystals in each well were dissolved in 180 μl DMSO. Absorbance at 590 nm was measured using a μ Quant, BioTek Instruments microplate reader.

Measurement of Intracellular Cu(I) Using BCA

Cells were grown in a sterile T-75 flask supplemented with complete DMEM medium (high glucose, fetal bovine serum-10%, antibiotics penicillin, and streptomycin (pen strep)- 5%, and L-glu-5%) in an incubator at 37 °C with 5% CO_2. The cells (105) were seeded in a six-well plate and kept in the incubator for 2–3 days to attach the cells; a 70–80% cell density was obtained in each well. Then the medium was replaced with fresh DMEM (2 mL). The cells were further treated with Cu(II) and the ATSM–Cu(II) complex for 0.5 h, 1 h, 3 h, 6 h, and 24 h. 2 mM stock solutions of Cu(II) and ATSM–Cu(II) were used. Hence, during the ATSM–Cu(II) treatment, the medium contained 0.5% DMSO. The final concentration of Cu(II) or ATSM–Cu(II) in each well was 10 μM. For normoxic conditions, the cells were incubated for the required time point at 37 °C and with 5% CO_2. For the hypoxia conditions, the plates were kept in a box containing hypoxic bags for 2 h before the treatment and again for the required time point after the treatment. After the treatment, the medium was removed from the wells, and cells were washed (2–3 times) with sterile PBS. Cell lysis buffer -RIPA buffer (300 μL) was added to the wells and shaken at 4 °C for 10 minutes. Then 300 μL of a solution from the BCA protein assay kit were added to the wells, and finally, 1.5 mL samples were collected into Eppendorf tubes. Each sample was warmed at 50 °C for 15 minutes, then covered with aluminium foil. After half an hour, the formation of Cu(I)–$(BCA)_2$ was detected at 562 nm using UV-Visible spectroscopy.

Radioactive Copper Experiments

^{64}Cu(II) stock was prepared in 0.2 M glycine buffer (pH- 5.5). ATSM–^{64}Cu(II) was prepared by adding ^{64}Cu(II) (469.5 μL) into the ATSM ligand dissolved in DMSO (3.84 mM, 365 μL). The stock solution was then diluted using glycine buffer to obtain the required activity for ATSM–^{64}Cu(II) in the desired volume. The complexation ratio was determined by HPLC, where both the UV and the gamma emission were detected, it was found that 95% of ^{64}Cu(II) was complexed to ATSM ligand.

HEK-293 and MCF-7 cells were grown in 6-well plates with 3 ml of DMEM high glucose (10% FBS, 1% PNSN, and 1% L-Glu) for 3 days until each well reached 85–90% confluency. Then the medium was removed from each well and replaced with 2 ml fresh medium. Finally, 150 μl 5 μCi of ^{64}Cu(II) or ATSM–^{64}Cu(II) was added into each well. For the hypoxic conditions, we added an anaerobic atmosphere generation bag to the box and closed it with a lid and paraffin. Under normoxic conditions, the cells were incubated for a full day at 37 °C and 5% CO_2. Under hypoxic conditions, however, the plates were at 37 °C and with 7–15% of CO_2 and 0.1% oxygen. After the treatment for the specific time intervals (1 h and 3 h), the medium was removed, and the cells were washed with PBS (4 ml). The cells were lysed using RIPA lysis buffer (300 μl) and then scraped. Finally, 300 μl of PBS was added, and cells were removed and measured for radioactivity using a gamma counter. All the

measurements were taken after fixing with a detector efficiency of 100%.

Western Blot Experiments

The cell lines cultures used for testing were grown in cell culture flasks and incubated at 37 °C with 5% CO_2 for a few days. After incubation, the culture was washed with cold PBS and lysed by adding RIPA Buffer. The samples containing 50 μg of total protein from each cell line were separated by SDS-PAGE and transferred to a nitrocellulose membrane using a transfer apparatus according to the manufacturer's protocols (Bio-Rad). After incubation with 3% milk solution in TBST (10 mM Tris, pH 8.0, 150 mM NaCl, 0.5% Tween 20) for 60 min, the membrane was incubated with antibodies against human CTR1 (GeneTex SLC314, 1:1000) or Actin DSHB JLA20, 1:500) at 4 °C over night. The membrane was washed with TBST three times for 10 min and incubated with a 1:20000 dilution of peroxidase-conjugated secondary antibody for 60 min. The blot was washed with TBST three times for 10 min and developed with the ECL system (Bio-Rad) according to the manufacturer's protocols.

Acknowledgments

G.W. was partly supported by a Colman-Soref postdoctoral fellowship. This work was supported by ERC-STG grant no. 754365.

Conflict of Interest

The authors declare no conflict of interest.

Keywords: ATSM–Cu(II) · copper toxicity · cancer · copper homeostasis

[1] a) M. A. Feitelson, A. Arzumanyan, R. J. Kulathinal, S. W. Blain, R. F. Holcombe, J. Mahajna, M. Marino, M. L. Martinez-Chantar, R. Nawroth, I. Sanchez-Garcia, D. Sharma, N. K. Saxena, N. Singh, P. J. Vlachostergios, S. Guo, K. Honoki, H. Fujii, A. G. Georgakilas, A. Bilsland, A. Amedei, E. Niccolai, A. Amin, S. S. Ashraf, C. S. Boosani, G. Guha, M. R. Ciriolo, K. Aquilano, S. Chen, S. I. Mohammed, A. S. Azmi, D. Bhakta, D. Halicka, W. N. Keith, S. Nowsheen, *Semin. Cancer Biol.* **2015**, *35 Suppl*, S25–S54; b) J. L. Tatum, G. J. Kelloff, R. J. Gillies, J. M. Arbeit, J. M. Brown, K. S. Chao, J. D. Chapman, W. C. Eckelman, A. W. Fyles, A. J. Giaccia, R. P. Hill, C. J. Koch, M. C. Krishna, K. A. Krohn, J. S. Lewis, R. P. Mason, G. Melillo, A. R. Padhani, G. Powis, J. G. Rajendran, R. Reba, S. P. Robinson, G. L. Semenza, H. M. Swartz, P. Vaupel, D. Yang, B. Croft, J. Hoffman, G. Liu, H. Stone, D. Sullivan, *Int. J. Radiat. Biol.* **2006**, *82*, 699–757.

[2] J. M. Brown, A. J. Giaccia, *Cancer Res.* **1998**, *58*, 1408–1416.

[3] a) B. Muz, P. de la Puente, F. Azab, A. K. Azab, *Hypoxia (Auckl)* **2015**, *3*, 83–92; b) M. Hockel, K. Sclenger, B. Aral, M. Mitze, U. Schaffer, P. Vaupel, *Cancer Res.* **1996**, *56*, 4509–4515; c) P. Vaupel, A. Mayer, *Cancer Metastasis Rev.* **2007**, *26*, 225–239.

[4] a) A. S. Cowburn, D. Macias, C. Summers, E. R. Chilvers, R. S. Johnson, *Elife* **2017**, *6*; b) M. C. Simon, L. Liu, B. C. Barnhart, R. M. Young, *Annu. Rev. Physiol.* **2008**, *70*, 51–71; c) E. Hernandez-Gerez, I. N. Fleming, S. H. Parson, *Cell Death Dis.* **2019**, *10*, 1-8.; d) N. N. Nalivaeva, E. A. Rybnikova, *Fron. Neurosci.* **2019**, *13*.

[5] A. W. Fyles, M. Milosevic, R. Wong, M.-C. Kavanagh, M. Pintilie, A. Sun, W. Chapman, W. Levin, L. Manchul, T. J. Keane, R. P. Hill, *Radiother. Oncol.* **1998**, *48*, 149–156.

[6] J. R. Ballinger, *Semin. Nucl. Med.* **2001**, *31*, 321–329.

[7] a) L. H. Gray, A. D. Conger, M. Ebert, S. Hornsey, O. C. Scott, *Br. J. Radiol.* **1953**, *26*, 638–648; b) J. M. Brown, *Methods Enzymol.* **2007**, *435*, 297–321; c) F. Wang, R. Luo, H. Xin, Y. Zhang, B. J. Cordova Wong, W. Wang, J. Lei, *Biomaterials* **2020**, *263*, 120330.

[8] a) R. A. Abdo, F. Lamare, P. Fernandez, M. Bentourkia, *Australas. Phys. Eng. Sci. Med.* **2019**, *42*, 981–993; b) I. Tachibana, Y. Nishimura, T. Shibata, S. Kanamori, K. Nakamatsu, R. Koike, T. Nishikawa, K. Ishikawa, M. Tamura, M. Hosono, *J. Radiat. Res.* **2013**, *54*, 1078–1084; c) S. T. Lee, A. M. Scott, *Semin. Nucl. Med.* **2007**, *37*, 451–461; d) S. Kizaka-Kondoh, H. Konse-Nagasawa, *Cancer Sci.* **2009**, *100*, 1366–1373; e) J. G. Rajendran, D. L. Schwartz, J. O'Sullivan, L. M. Peterson, P. Ng, J. Scharnhorst, J. R. Grierson, K. A. Krohn, *Clin. Cancer Res.* **2006**, *12*, 5435–5441.

[9] J. G. Rajendran, D. A. Mankoff, F. O'Sullivan, L. M. Peterson, D. L. Schwartz, E. U. Conrad, A. M. Spence, M. Muzi, D. G. Farwell, K. A. Krohn, *Clin. Cancer Res.* **2004**, *10*, 2245–2252.

[10] a) P. J. Blower, J. S. Lewis, J. Zweit, *Nucl. Med. Biol.* **1996**, *23*, 957–980; b) Y. Fujibayashi, H. Taniuchi, Y. Yonekura, H. Ohtani, J. Konishi, A. Yokoyama, *J. Nucl. Med.* **1997**, *38*, 1155–1160; c) J. L. Dearling, J. S. Lewis, G. E. Mullen, M. T. Rae, J. Zweit, P. J. Blower, *Eur. J. Nucl. Med.* **1998**, *25*, 788–792; d) A. L. Vavere, J. S. Lewis, *Dalton Trans.* **2007**, 4893–4902; e) D. W. McCarthy, L. A. Bass, P. D. Cutler, R. E. Shefer, R. E. Klinkowstein, P. Herrero, J. S. Lewis, C. S. Cutler, C. J. Anderson, M. J. Welch, *Nucl. Med. Biol.* **1999**, *26*, 351–358; f) J. P. Holland, J. C. Green, J. R. Dilworth, *Dalton Trans.* **2006**, 783–794.

[11] a) S. Y. Park, W. J. Kang, A. Cho, J. R. Chae, Y. L. Cho, J. Y. Kim, J. W. Lee, K. Y. Chung, *PLoS One* **2015**, *10*, e0131083; b) M. Colombie, S. Gouard, M. Frindel, A. Vidal, M. Cherel, F. Kraeber-Bodere, C. Rousseau, M. Bourgeois, *Front. Med. (Lausanne)* **2015**, *2*, 58; c) A. E. Hansen, A. T. Kristensen, J. T. Jorgensen, F. J. McEvoy, M. Busk, A. J. van der Kogel, J. Bussink, S. A. Engelholm, A. Kjaer, *Radiat. Oncol.* **2012**, *7*, 89.

[12] a) Z. Xiao, P. S. Donnelly, M. Zimmermann, A. G. Wedd, *Inorg. Chem.* **2008**, *47*, 4338–4347; b) G. R. Walke, S. Ruthstein, *ACS Omega* **2019**, *4*, 12278–12285.

[13] J. L. Dearling, A. B. Packard, *Nucl. Med. Biol.* **2010**, *37*, 237–243.

[14] a) E. Gaggelli, H. Kozlowski, D. Valensin, G. Valensin, *Chem. Rev.* **2006**, *106*, 1995–2044; b) G. R. Walke, S. Rapole, P. P. Kulkarni, *Inorg. Chem.* **2014**, *53*, 10003–10005; c) G. R. Walke, D. S. Ranade, A. M. Bapat, R. Srikanth, P. P. Kulkarni, *ChemistrySelect* **2016**, *1*, 3497–3501.

[15] a) J. O. Pinho, J. D. Amaral, R. E. Castro, C. M. Rodrigues, A. Casini, G. Soveral, M. M. Gaspar, *Nanomedicine (Lond)* **2019**, *14*, 835–850; b) N. Zuin Fantoni, Z. Molphy, C. Slator, G. Menounou, G. Toniolo, G. Mitrikas, V. McKee, C. Chatgilialoglu, A. Kellett, *Chemistry* **2019**, *25*, 221–237; c) O. Krasnovskaya, A. Naumov, D. Guk, P. Gorelkin, A. Erofeev, E. Beloglazkina, A. Majouga, *Int. J. Mol. Sci.* **2020**, *21*.

[16] R. Anjum, D. Palanimuthu, D. S. Kalinowski, W. Lewis, K. C. Park, Z. Kovacevic, I. U. Khan, D. R. Richardson, *Inorg. Chem.* **2019**, *58*, 13709–13723.

[17] A. L. Vavere, J. S. Lewis, *Nucl. Med. Biol.* **2008**, *35*, 273–279.

[18] a) L. A. Yatsunyk, A. C. Rosenzweig, *J. Biol. Chem.* **2007**, *282*, 8622–8631; b) A. J. Brenner, E. D. Harris, *Anal. Biochem.* **1995**, *226*, 80–84.

[19] J. S. Lewis, D. W. McCarthy, T. J. McCarthy, Y. Fujibayashi, M. J. Welch, *J. Nuc. Med.* **1999**, *40*, 177–183.

[20] C. Stefani, Z. Al-Eisawi, P. J. Jansson, D. S. Kalinowski, D. R. Richardson, *J. Inorg. Biochem.* **2015**, *152*, 20–37.

Manuscript received: February 22, 2021
Revised manuscript received: March 8, 2021